ACADEMIC PRESS

Archives of Biochemistry and Biophysics 401 (2002) 145–154

ABB

www.academicpress.com

Diversity of properties among catalases

Jacek Switala and Peter C. Loewen*

Department of Microbiology, University of Manitoba, Winnipeg, Manitoba, Canada R3T 2N2

Received 22 January 2002, and in revised form 4 March 2002

Abstract

Catalases from 16 different organisms including representatives from all three phylogenetic clades were purified and characterized to provide a comparative picture of their respective properties. Collectively the enzymes presented a diverse range of activities and properties. Specific activities ranged from 20,700 to 273,800 units per milligram of protein and maximal turnover rates ranged from 54,000 to 833,000 per second. The effective concentrations of common catalase inhibitors, cyanide, azide, hydroxylamine, aminotriazole, and mercaptoethanol, varied over a 100- to 1000-fold concentration range, and a broad range of sensitivities to heat inactivation was observed. Michaelis–Menten kinetics were approximately followed only at the low substrate concentrations. At high H_2O_2 concentrations, inactivation of small-subunit enzymes resulted in lower velocities than what were predicted, whereas large-subunit enzymes had velocities higher than predicted. Kinetic constants such as K_m and V_{max} for catalases must be labeled as "apparent."

Keywords: Catalase; Diversity; Enzymology; Structure–function

Catalases are protective enzymes responsible for the degradation of hydrogen peroxide before it can damage cellular components (reaction (1)). They are present in virtually all aerobic organisms and many anaerobic organisms. The catalatic reaction takes place in two steps with the first hydrogen peroxide molecule oxidizing the heme to an oxyferryl species in which one oxidation equivalent is removed from the iron and one from the porphyrin ring to generate a porphyrin cation radical (reaction (2)). The second hydrogen peroxide is then used as a reductant of compound I to regenerate the resting state enzyme, water, and oxygen (reaction (3)).

$$2H_2O_2 \rightarrow 2H_2O + O_2 \quad (1)$$

$$\mathrm{Enz(Por - Fe^{III}) + H_2O_2} \rightarrow \mathrm{Cpd\ I(Por^{+\cdot} - Fe^{IV} = O) + H_2O} \quad (2)$$

$$\mathrm{Cpd\ I(Por^{+\cdot} - Fe^{IV} = O) + H_2O_2} \rightarrow \mathrm{Enz(Por - Fe^{III}) + H_2O + O_2}. \quad (3)$$

Catalase activity is exhibited by a number of different proteins including monofunctional heme-containing catalases, bifunctional catalase-peroxidases, and non-heme catalases. In addition, low levels of catalase activity are found in many heme containing proteins not normally considered to be catalases. The former category of monofunctional heme-containing catalases will serve as the focus of this communication.

Catalases have been studied biochemically for over 100 years [1] with the result that examples of the enzyme have been isolated and characterized from many different organisms. Of these, seven have had their crystal structures published including the enzymes from bovine liver (BLC)[1] [2,3], *Penicillium vitale* (PVC) [4,5], *Micrococcus lysodeikticus*, (MLC) [6], *Proteus mirabilis* (PMC) [7], *Escherichia coli* (HPII) [8,9], *Saccharomyces cerevisiae* (CATA) [10,11], and human erythrocytes (HEC) [12,13]. In addition, a preliminary report of the crystallization of an eighth catalase, CatF from *Pseudomonas syringae*, has appeared [14] and the atomic coordinates are available from the authors. Moreover, the sequences of catalase genes from more than 200

* Corresponding author. Fax: +204-474-7603.
E-mail address: peter_loewen@umanitoba.ca (P.C. Loewen).

[1] *Abbreviations used:* BLC, bovine liver crystal structure; HPII, *Escherichia coli* crystal structure; CATA, *Saccharomyces cerevisiae* crystal structure; YPD, yeast potato dextrose; M-M, Michaelis–Menten.

0003-9861/02/$ - see front matter
PII: S0003-9861(02)00049-8

organisms are available, providing an extensive database for comparison.

Among the enzymes purified and characterized, a wide range of biochemical and kinetic properties have been reported. Comparison of these data has been complicated by the use of different assay techniques and conditions. Furthermore, a value for the Michaelis constant K_m has frequently been reported without qualification despite the fact that the enzyme does not follow Michaelis–Menten kinetics. Given the possibility of rationalizing structure with function, it has become critical that a consistent and comparative set of data describing catalases be prepared in order to allow a rational comparison of physiological differences with structural changes. This paper reports the first side by side characterization of 16 catalases from a range of organisms and a comparison, where possible, to available structures.

Materials and methods

Source of catalases. The strains and plasmids used in this work are listed in Table 1. The catalases from *M. luteus*, *P. mirabilis*, *S. marcescens*, and *Xanthomonas campestris* were prepared directly from the strains indicated. The catalases from *Bacteroides fragilis*, *Bordetella pertussis*, *Brucella abortus, E. coli*, *Helicobacter pylori*, *Listeria seeligeri*, *Pseudomonas aeruginosa*, and *P. syringae* were expressed from the relevant plasmids in the catalase deficient host, UM255, grown in shaken batch culture in Luria broth containing 10 g/L tryptone, 5 g/L yeast extract, and 5 g/L NaCl usually for 16 h at 37 °C except that the *P. syringae catF* clone was grown at 28 °C for 22 h. The catalases from *Aspergillus niger* and bovine liver were from Sigma and human erythrocyte catalase was from Calbiochem. The *S. cerevisiae* catalase CatA was expressed in the catalase deficient yeast strain GC1-8B grown in YPD medium as described [11].

Activity, protein, and spectral determination. Catalase activity was determined by the method of Rørth and Jensen [15] in a Gilson oxygraph equipped with a Clark electrode. One unit of catalase is defined as the amount that decomposes 1 μmol of H_2O_2 in 1 min in a 60 mM H_2O_2 solution at pH 7.0 at 37 °C. Initial rates of oxygen evolution were used to determine the turnover rates to minimize the inactivation caused by high $[H_2O_2]$ [16]. Protein was estimated according to the methods outlined by Layne [17]. Gel electrophoresis of proteins was carried out on SDS–polyacrylamide gels as previously described [18,19]. Absorption spectra were obtained using a Milton Roy MR3000 spectrophotometer. Samples were dissolved in 50 mM potassium phosphate, pH 7.0.

Enzyme purification. Bacterial cells were broken using a French pressure cell and yeast cells were broken using a Braun homogenizer. Purification of catalase from all extracts was essentially as described [20] with the following modifications. Following resuspension of the ammonium sulfate fraction, any preparations that were not adversely affected by heat treatment were heated at 50 °C for 15 min followed by centrifugation prior to chromatography on DEAE–cellulose (Whatman). Enzymes that did not bind to DEAE–cellulose were purified using hydroxylapatite (Bio-Rad). A summary of which enzymes were treated by these alternate procedures is contained in Table 2. The commercial catalases were dialyzed against 50 mM potassium phosphate buffer, pH 7, and any resulting precipitate was removed

Table 1
Bacterial strains and plasmids

Name	Genotype and source	
A. Strains		
Escherichia coli UM255	*pro leu rpsL hsdM hsdR endI lacY katG2 katE12::*Tn*10 recA* [27]	
Micrococcus luteus	ATCC 4698	
Proteus mirabilis	University of Manitoba Collection	
Saccaromyces cerevisiae GC1-8B	No. 578 a, leu2 trp1 ura3 ctt1-1 cta1-2 [11]	
Serratia marcescens	University of Manitoba Collection	
Xanthomonas campestris XpHR	[28]	
Name	Gene encoded	Source
B. Plasmids		
pFD568	*Bacteroides fragilis katB*	[29]
pBkat13	*Bordetella pertussis katA*	[30]
pCAT6	*Brucella abortus kat*	[31]
pkatE72	*Escherichia coli katE*	[32]
pSO100	*Helicobacter pylori katA*	[33]
pAHA1	*Listeria seeligeri katA*	[34]
pSMB1	*Pseudomonas aeruginosa katB*	[35]
pEC3E56	*Pseudomonas syringae catF*	[36]
YEp352E	*Saccharomyces cerevisiae catA*	[11]

Table 2
Catalase Purification

Source	Growth temp (°C)	Heat[a]	Column[b]	Extraction[c]	SA[d]	Clade
A. niger	na[e]	na	na	na	21,400	II
B. fragilis	37	+	DEAE	+	69,100	III
B. pertussis	37	–	DEAE	+	225,000	III
Bovine liver	na	na	na	na	91,800	III
B. abortus	37	–	DEAE	–	145,800	III
E. coli	37	+	DEAE	+	20,700	II
H. pylori	37	–	HTP	–	61,400	III
Human erythrocyte	na	na	na	na	273,800	III
L. seeligeri	37	+	DEAE+HTP	–	89,300	I
M. luteus	28	–	DEAE	+	109,100	III
P. mirabilis	37	–	DEAE	+	160,000	III
P. aeruginosa	37	–	HTP	–	71,800	III
P. syringae	28	–	HTP	–	84,600	I
S. cerevisiae	28	–	HTP	+	116,100	III
S. marscesens	37	+	DEAE	+	98,900	III
X. campestris	28	+	HTP	–	99,900	III

[a] Protein was heated at 50 °C for 15 min prior to ion-exchange chromatography.
[b] Ion-exchange resin: DEAE, DEAE–Cellufine; HTP hydroxyapatite.
[c] Extraction was with ethanol:chloroform in a mixture ethanol:chloroform:protein solution of 5:3:10 (v v v).
[d] SA, specific activity expressed in units/mg protein.
[e] na, not applicable because enzyme purchased.

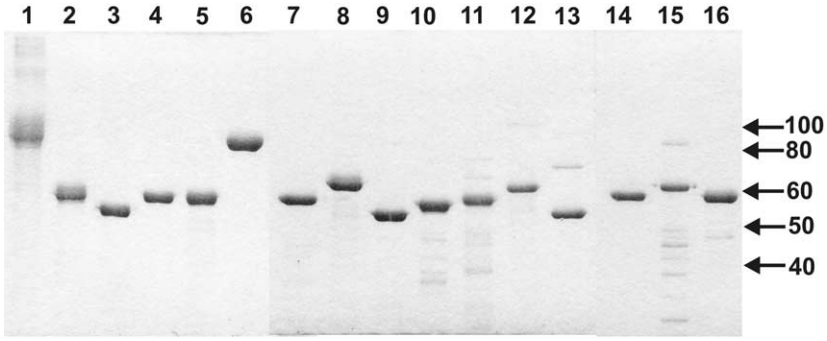

Fig. 1. SDS–polyacrylamide analysis of purified catalases. Samples were run on a 8% polyacrylamide gel. The locations and sizes (in kDa) of size markers are indicated by the arrows. The sources of the catalases in the various lanes are as follows: (lane 1) *A. niger*, (lane 2) *B. fragilis*, (lane 3) *B. pertussis*, (lane 4) bovine liver, (lane 5) *B. abortus*, (lane 6) *E. coli*, (lane 7) *H. pylori*, (lane 8) *L. seeligeri*, (lane 9) *P. aeruginosa*, (lane 10) *P. syringae*, (lane 11) *S. cerevisiae*, (lane 12) *S. marcescens*, (lane 13) *X. campestris*, (lane 14) human erythrocytes, (lane 15) *M. luteus*, and (lane 16) *P. mirabilis*.

by centrifugation. Based on spectral analysis, the catalases from *E. coli* and *A. niger* contained heme d and all others contained heme b (data not shown). Samples of all proteins used in this study were analyzed on SDS–polyacrylamide gels (Fig. 1).

Results

Purification

The catalases were all purified following the same basic protocol [20] which involves breaking the cells using a French press, streptomycin sulfate treatment, ammonium sulfate precipitation, and ion-exchange chromatography, usually on DEAE–cellulose. A number of supplementary steps were introduced for individual enzymes based on differing properties. These are summarized in Table 2. For example, hydroxylapatite was used when an enzyme did not bind to DEAE–cellulose. The heat treatment and ethanol–chloroform extraction were employed only after testing on a small scale that the enzyme was not inactivated and was purified further as a result of the treatment. The only exceptions to this were the three enzymes, from human erythrocytes, bovine liver, and *A. niger*, that were obtained commercially.

Kinetic comparison

A comparison of the specific activities of 16 catalases, all assayed under the same conditions, reveals a very

broad range from 20,700 to 273,800 units per milligram of protein (Table 2). Catalase has long been recognized as an enzyme with a rapid turnover rate and the maximum observed velocities range from 54,000 to 833,000 reactions per second (Table 3) corroborate this notoriety. The H_2O_2 concentrations at which 50% of maximal activity is attained (apparent K_m) is also included and reveal a similar broad variation from 38 to 600 mM.

The classical terms, V_{max}, k_{cat}, and K_m, cannot be directly applied to the observed data because catalases do not exhibit Michaelis–Menten kinetics over the complete substrate concentration range (Fig. 2) and because of the two-step nature of the catalatic reaction [1]. However, at H_2O_2 concentrations below 200 mM, all small-subunit catalases do exhibit a Michaelis–Menten-like dependence of velocity on H_2O_2 concentration, and these data were used to calculate theoretical K_m and V_{max} values (Table 3). The theoretical dependence of velocity on substrate concentration calculated using the Michaelis–Menten equation are plotted in Fig. 2 (dashed lines) for comparison with the observed data. There is good correlation between the theoretical and observed curves at low $[H_2O_2]$, but the correlation ends as the velocity abruptly stops increasing and begins to decrease at higher $[H_2O_2]$, a result of enzyme inactivation caused by the reactive substrate, H_2O_2. The data shown for *B. fragilis* catalase (Fig. 2A) are typical of the observed and theoretical curves for the 13 other small-subunit enzymes in the comparison. The data for the *P. mirabilis* catalase are also shown (Fig. 2B), because of the exceptional observed and theoretical k_{cat} values of 0.83 and 1.63×10^6 molecules of H_2O_2 degraded per second. While the divergence from Michaelis–Menten kinetics in the small-subunit enzymes is the result of inactivation caused by H_2O_2-induced damage, the sensitivity to damage is quite variable. The enzymes from *P. aeruginosa* and *L. seeligeri* exhibited maximum activity at 0.2 M H_2O_2 whereas those from *P. mirabilis* and *P. syringae* reached maximum velocity only at 1 M H_2O_2.

The kinetic curves of the two large-subunit catalases from *A. niger* and *E. coli* (Fig. 2C and D) differ from those of the small-subunit enzymes. The enzymes are relatively insensitive to the damaging properties of H_2O_2, and the velocities continue to increase as the H_2O_2 concentrations rise above 1 M. The *E. coli* enzyme begins to exhibit a reduction in velocity above 3 M H_2O_2, and the velocity of the *A. niger* enzyme continues to increase up to 5 M H_2O_2. Theoretical K_m and V_{max} values calculated from the data below 400 mM $[H_2O_2]$ (Table 3) give rise to theoretical Michaelis–Menten curves that lie below the observed data (Fig. 2C and D). The divergence is greater for the *E. coli* enzyme and is clearly evident in the nonlinear double-reciprocal plot in the inset to Fig. 2C. Unlike the spectroscopic assay for catalase activity which is restricted to lower peroxide concentrations, the oxygraph assay used for these studies allows the direct determination of catalase activity at high-peroxide concentrations without the need for extrapolation, but 5 to 6 M peroxide is the practical upper limit because stock H_2O_2 has a concentration of 9 to 11 M.

Effect of inhibitors

Catalases are sensitive to a number of compounds that interact with the active-site heme including cyanide, azide, hydroxylamine, aminotriazole, and mercaptoethanol. The concentrations of inhibitor required for

Table 3
Observed and calculated kinetic parameters

Source	Observed		Calculated[a]		
	V_{max}[b]	$[H_2O_2]@V_{max}/2$, mM	V_{max}[b]	K_m, mM	k_{cat}/K_m s^{-1} M^{-1}
A. niger	315,000	599	277,000	465	0.60×10^6
B. fragilis	241,000	128	380,000	279	1.36×10^6
B. pertussis	424,000	88	595,000	154	3.86×10^6
Bovine liver	181,000	93	212,000	93	2.28×10^6
B. abortus	380,000	84	562,000	174	3.23×10^6
E. coli HPII	151,000	312	70,000	64	1.09×10^6
H. pylori	250,000	108	272,000	127	2.14×10^6
Human erythrocyte	548,000	81	587,000	80	7.34×10^6
L. seeligeri	133,000	49	214,000	111	1.93×10^6
M. luteus	284,000	147	313,000	152	2.06×10^6
P. mirabilis	833,000	200	1,630,000	537	3.04×10^6
P. aeruginosa	54,000	38	71,000	67	1.06×10^6
P. syringae	238,000	82	281,000	92	3.05×10^6
S. cerevisiae	278,000	94	355,000	125	2.84×10^6
S. marscesens	228,000	180	243,000	228	1.07×10^6
X. campestris	244,000	64	279,000	77	3.62×10^6

[a] Calculated constants from extrapolation of $1/V$ vs $1/[H_2O_2]$ for $[H_2O_2] < 400$ mM.
[b] Units of V_{max} are μmol H_2O_2 μmol heme^{-1} s^{-1}.

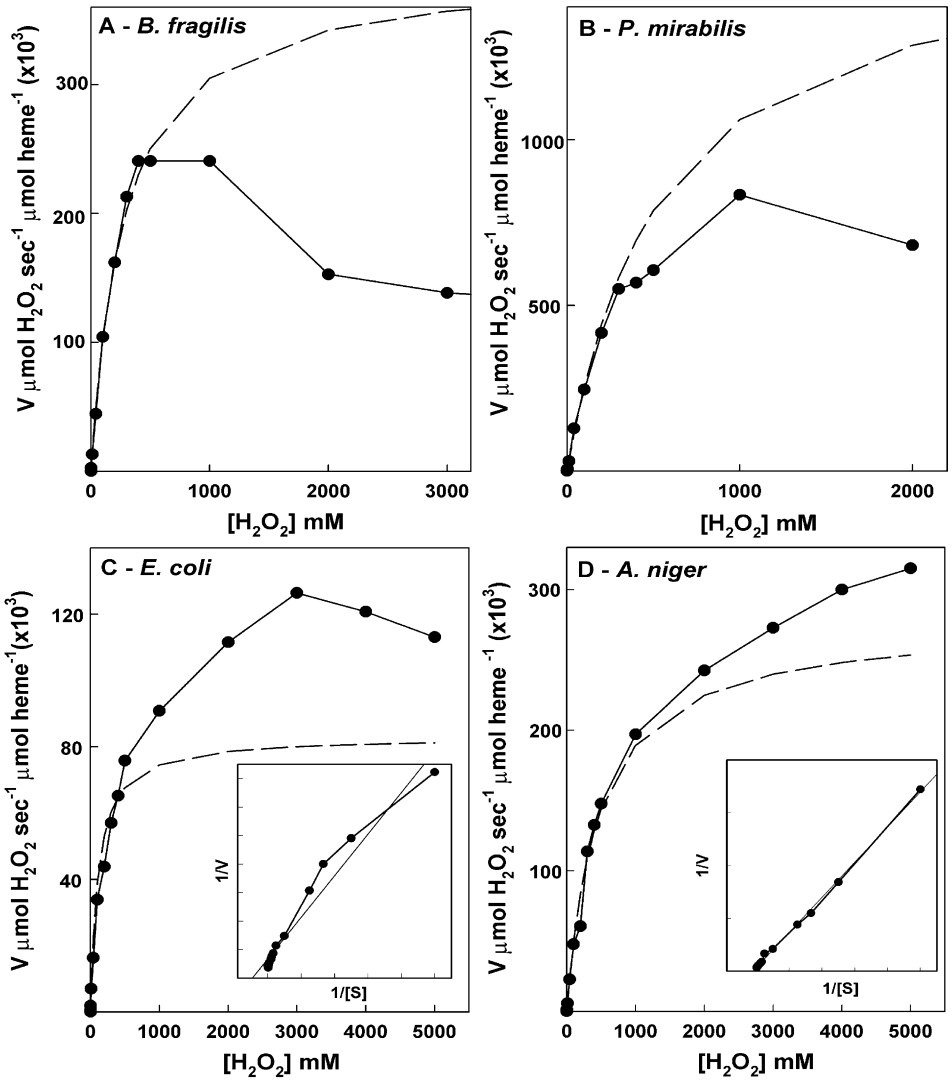

Fig. 2. Dependence of enzyme velocity on H_2O_2 concentration. In all panels the solid line represents the observed data and the dashed line represents the theoretical Michaelis–Menten curve calculated from constants determined at low H_2O_2 concentration (Table 3). The enzymes included are the small-subunit enzymes from (A) *B. fragilis* and (B) *P. mirabilis* and the large-subunit enzymes from (C) *E. coli* and (D) *A. niger*. Note the differences in the scales of the velocity axes. The insets in C and D are the double-reciprocal plots that illustrate the divergence from Michaelis–Menten kinetics even at low H_2O_2 concentrations for HPII. All assays were repeated in triplicate and the results were averaged.

50% inhibition are included in Table 4, and the times required for 50% inactivation by 2-mercaptoethanol are included in Table 5. In all cases, there is a wide range of concentrations or times required for 50% inhibition. The most striking are the greater than 1000-fold range of effectiveness for aminotriazole and hydroxylamine (from 1 to >1000 mM and 0.2 to 200 μM, respectively. Examples of the kinetics of inactivation for a few of the enzymes are shown in Figs. 3 and 4 to illustrate the extreme differences.

Heat sensitivity

Catalases have been shown to be quite heat stable with the BLC having a T_m of 56 °C and the HPII from *E. coli* having a T_m of 82 °C [21]. The catalases in this study were incubated at 65 °C and the times required for 50% inactivation were determined (Table 5). A broad range of times from 0.1 to 720 min were observed indicating to a very broad range of stabilities. The extreme differences in sensitivity to heat among the enzymes are illustrated in Fig. 4.

Discussion

The core sequences in catalases presented a remarkable level of conservation among more than 70 [22] examples and continue to do so among the more than 200 sequences now available (data not shown). Paralleling

Table 4
Effectiveness of various inhibitors

Source	Concentration at 50% inhibition[a]			
	NaCN, μM	NaN_3, μM	Aminotriazole, mM	NH_2OH, μM
A. niger	300	150	450	0.40
B. fragilis	60	15	> 1000	200
B. pertussis	35	1.0	500	4.0
Bovine liver	30	1.5	40	3.0
B. abortus	15	1.5	250	3.0
E. coli	9	130	> 1000	0.12
H. pylori	150	1.5	350	6.0
Human erythrocyte	20	1.5	30	2.0
L. seeligeri	25	1.0	90	0.35
M. luteus	60	1.5	> 1000	3.0
P. mirabilis	80	60	> 1000	100
P. aeruginosa	12	2.0	1.5	0.35
P. syringae	12	1.0	1.0	0.20
S. cerevisiae	35	1.5	60	2.0
S. marscesens	80	25	> 1000	200
X. campestris	15	1.0	2.0	0.30

[a] The enzyme was incubated with inhibitor for 1 min before adding H_2O_2.

Table 5
Sensitivity to 5 mM 2-mercaptoethanol and incubation at 65 °C

Source	Time to 50% inactivation (min) MSH	65 °C
A. niger	40	14
B. fragilis	10	5
B. pertussis	5	10
Bovine liver	2[a]	0.3
B. abortus	3	4
E. coli	40[b]	720
H. pylori	3	1
Human erythrocyte	3[a]	0.2
L. seeligeri	3[a]	1
M. luteus	49	6
P. mirabilis	6	14
P. aeruginosa	2[a]	0.05
P. syringae	0.25[a]	0.2
S. cerevisiae	1[a]	0.1
S. marscesens	3	12
X. campestris	0.25[a]	0.3

[a] Assayed in 1 mM 2-mercaptoethanol.
[b] Assayed in 10 mM 2-mercaptoethanol.

the sequence conservation is a conservation of structure among eight catalases from organisms as phylogenetically distinct as humans and bacteria. This extensive sequence and structural similarity suggested that many of the properties of these enzymes would be similar, but the data described in this paper reveal just the opposite; there are striking variations of 10 to 1000 times in specific activities, reaction velocities, sensitivity to damage by the substrate H_2O_2, and sensitivity to inactivation by inhibitors and heat. Explaining the structural bases for these different properties poses a real challenge.

The data presented here clearly demonstrate the point that catalases do not exhibit Michaelis–Menten kinetics and do not become saturated with substrate, a point that has been stressed recently [1]. At high H_2O_2 concentrations, small-subunit catalases exhibit lower velocities than predicted by the Michaelis–Menten (M-M) equation because of inactivation by H_2O_2. Large-subunit enzymes are not inactivated as easily and the observed velocities at high substrate concentrations are actually greater than predicted by the M-M equation. In the absence of inactivation, the small-subunit enzymes would probably exhibit rates faster than predicted by the M-M equation as well. Indeed, the data for *B. fragilis* (Fig. 2A) reveal a divergence to velocities faster than predicted by Michaelis–Menten at 300 to 400 mM H_2O_2 with inactivation becoming evident at 500 mM H_2O_2. Most catalase are characterized at low substrate con-

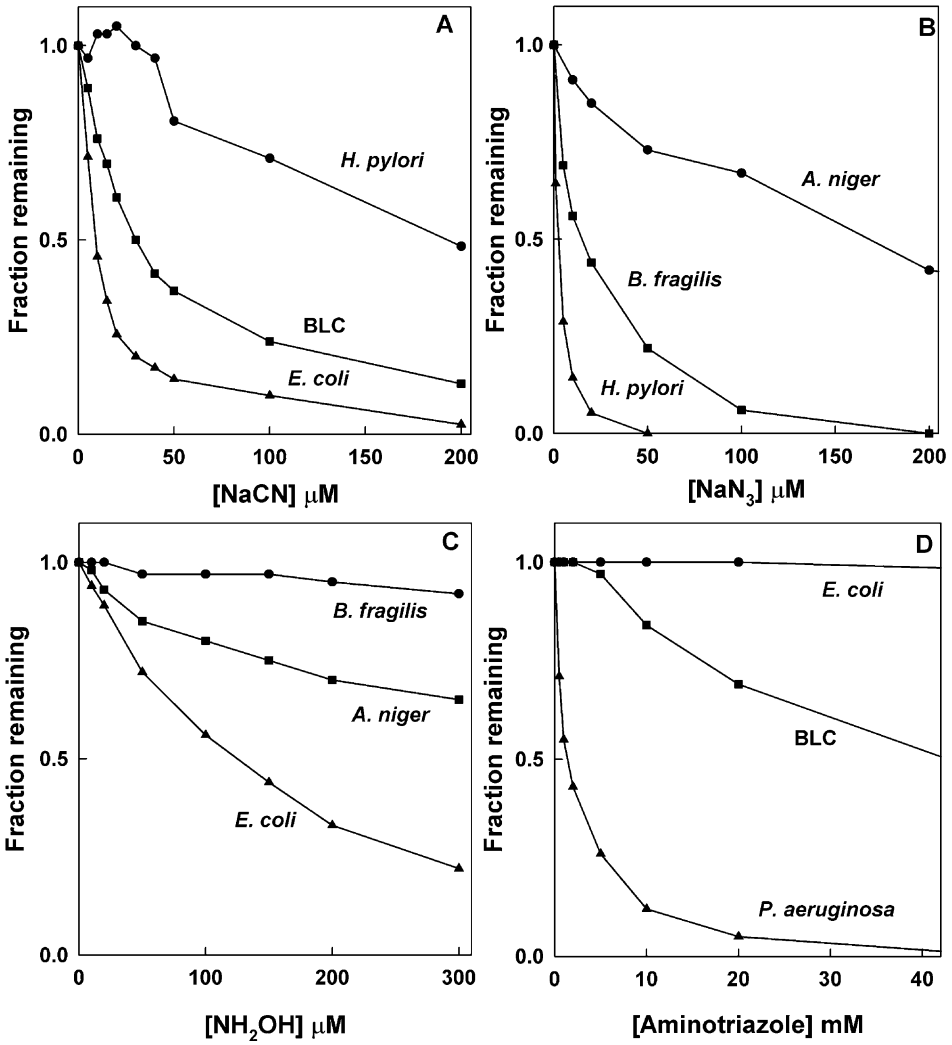

Fig. 3. Representative examples of the kinetics of inhibition by (A) NaCN, (B) NaN_3, (C) NH_2OH, and (D) aminotriazole. In each case the most and least sensitive enzymes from the group are compared with one that is representative of the remainder. All assays were repeated in triplicate and the results were averaged.

centrations where the data resemble M-M kinetics sufficiently well to be misleading, but the variation of observed K_m and V_{max} values from calculated values presented demonstrate the discrepancy. One other point worth noting is that specific activities of catalases are usually determined at substrate concentrations below the apparent K_m where there is great variation in velocity with substrate concentration, and this makes meaningful comparisons of literature data virtually impossible.

Passage of the substrate H_2O_2 through one or more channels to the deeply buried active site is essential for catalase activity, and subtle differences in the size or shape of the channels may influence substrate entry or product exhaust giving rise to some of the observed differences. There are three channels that have been implicated as potentially having a role in access to the active site. The perpendicular (relative to the plane of the heme) or main channel has long been considered to be the access channel and variants of yeast CATA mutated in residues lying in the channel [23] as well as molecular dynamics studies [24,25] support this idea. The lateral or minor channel was shown to be important, possibly as an inlet channel, in HPII [26] and in small-subunit enzymes [11]. More recently, a thermodynamic modeling of solvent flow through catalase has identified a third channel leading from the heme to the central cavity of the tetramer [25]. All three channels are quite narrow particularly as they approach the heme-containing active-site cavity, and this restricts accessibility to relatively small molecules, generally not much larger than H_2O_2.

In small-subunit enzymes, the first 20 Å of the perpendicular (or main) channel starting from the surface of the protein is funnel shaped presenting little obstacle

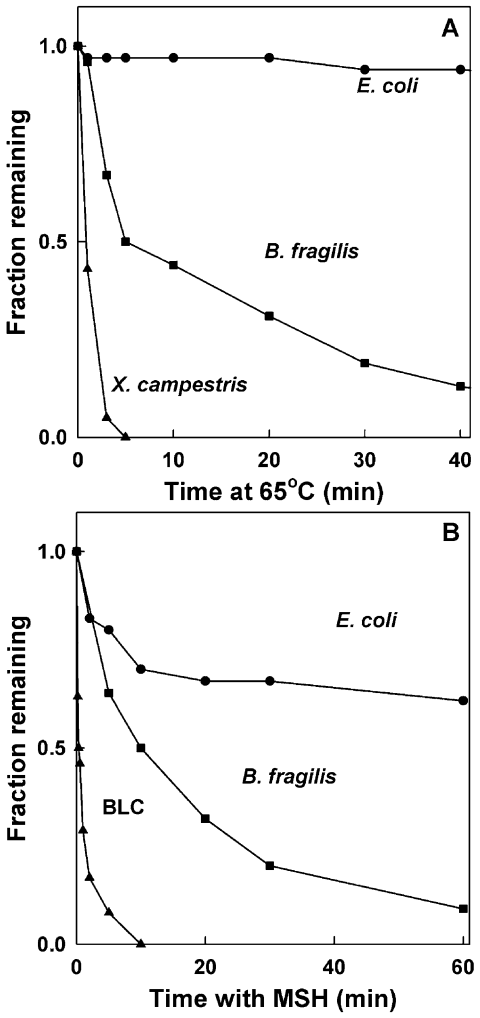

Fig. 4. Representative examples of sensitivity to (A) 2-mercaptoethanol and (B) heating at 65 °C. In each case, the most and least sensitive enzymes from the group are compared with one that is representative of the remainder. All assays were repeated in triplicate and the data were averaged.

to even large molecules (BLC in Fig. 5A). The next 15 Å of the channel extending from a conserved aspartate (No. 127 in BLC) to the heme is constricted, restricting access to only small molecules. This was predicted to be a region of the protein that would provide explanations for the differences in selectivity, but the residues that line this part of the channel are highly conserved both in identity and in location and do not provide obvious clues. For example, the sequences of the enzymes from *P. mirabilis* and *P. aeruginosa* are very similar, even including a methionine adjacent to the active-site histidine which can be oxidized, and yet the former has a very high turnover rate and is relatively insensitive to many inhibitors, whereas the latter has a low turnover rate but is highly sensitive to inhibitors.

The large-subunit enzymes present a very different structure in the upper part of the channel with the open funnel structure being replaced by an elongated, constricted, and possibly bifurcated channel involving the C-terminal domain of an adjacent subunit (Fig. 5B). Even this difference from small-subunit enzymes provides only a superficial explanation for the differences between large- and small-subunit enzymes. For example, the maximum turnover rates of HPII from *E. coli* and BLC are similar at 151,000 and 181,000 per second, respectively, but HPII requires a 10-fold higher H_2O_2 concentration (3 M compared to 0.3 M for BLC) to achieve its maximal rate. The extended and more constricted channel of HPII might explain the lower turnover rate but is inconsistent with the greater sensitivity of HPII to some inhibitors compared to BLC.

Like comparison of channel architectures, simple sequence comparisons are unlikely to provide clear explanations for the observed differences. Other factors such as inductive effects of residues surrounding the channels and the active site and flexibility in the protein must influence the reactivity and binding efficiencies of the different enzymes. Identifying such subtle factors is further complicated by the uncertainty in channel utilization. Until it is proven which channel or channels are used for inlet of substrate and exhaust of products, assignment of roles to specific residues will be difficult.

The differences in sensitivity to heat inactivation pose an even more complex problem. HPII from *E. coli* is the most resistant to heat denaturation, a property that was earlier attributed, in part, to the interweaving of the long N-terminal extensions with an adjacent subunit, but this can be only part of the explanation. The *A. niger* catalase has a similar long N-terminal sequence that should generate an interwoven structure, and yet it exhibits a temperature sensitivity similar to that of small-subunit enzymes with much shorter N-terminal extensions. Furthermore, the *P. syringae* CatF with the longest N-terminal extension among the small-subunit enzymes is one of the most heat-sensitive enzymes. Many interactions that stabilize the secondary, tertiary, and quaternary structure throughout the protein are likely involved in determining this property, and it is unlikely that simple sequence comparisons will provide the needed explanations.

On the other hand, one property that may be explainable at least in part is that of greater resistance to damage by H_2O_2 in large-subunit enzymes. All large-subunit enzymes so far characterized contain heme d, a *cis*-hydroxy spirolactone oxidized derivative of heme b, a modification that is self-catalyzed by the catalase. This controlled oxidation of heme b to heme d by large-subunit enzymes may serve to make the heme less sensitive to further damaging oxidation by H_2O_2, and this in turn makes the enzyme more resistant to peroxide damage.

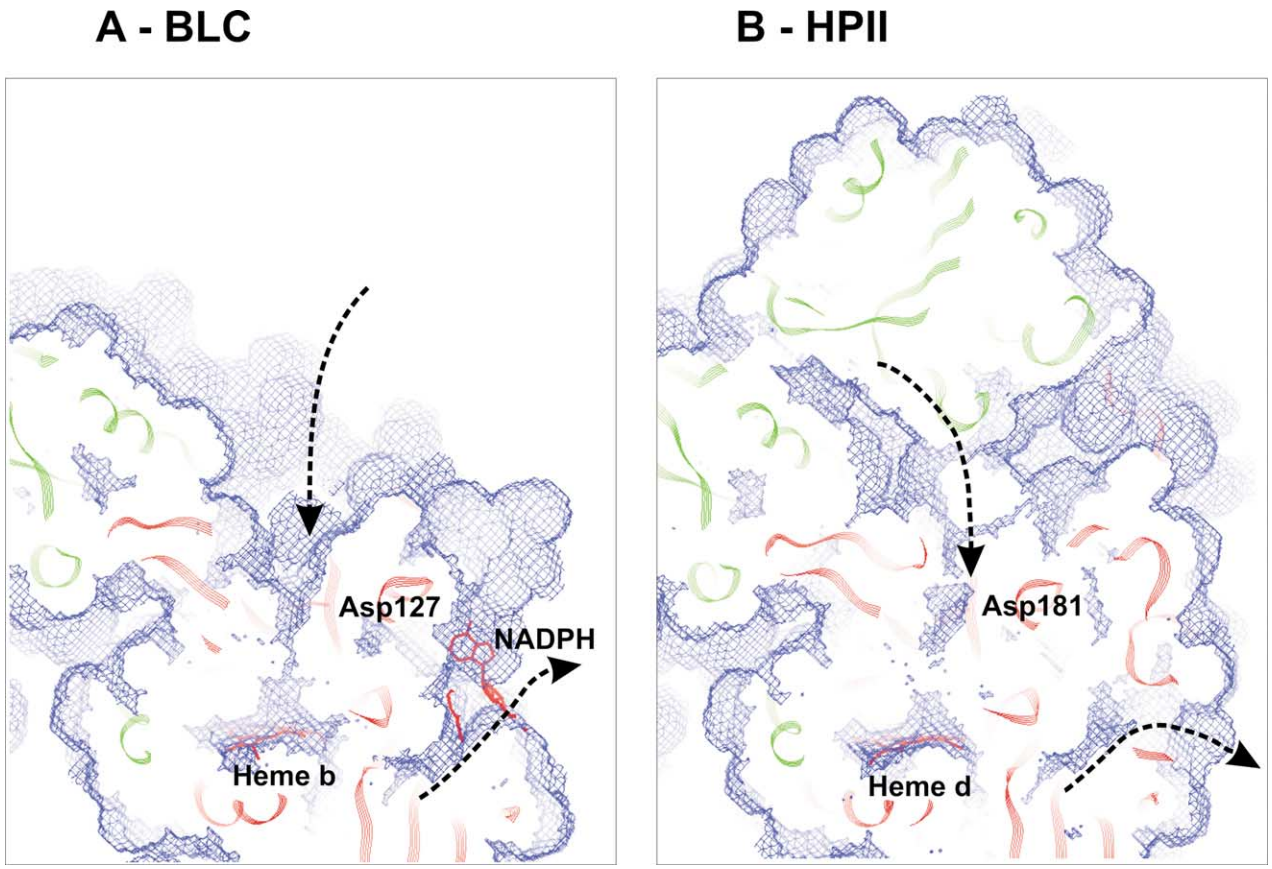

Fig. 5. Comparison of the perpendicular (main) and lateral channel structures leading to the active sites of a dimer of the small-subunit enzyme from bovine liver (BLC) and (B) a dimer of the large-subunit enzyme from *E. coli* HPII. The accessibility surfaces determined using VOIDOO [37] are shown as a blue lattice and are a reflection of what parts of the protein are accessible to a molecule about the size of water. A cross-section or slab of the protein is shown that contains "channels" leading to the heme active site that are accessible to the exterior of the protein. The dashed lines (the perpendicular channel arrow points down and the lateral channel arrow points to the right of the diagrams) are placed adjacent to the channels to orient the reader. The implication from the direction of the arrows, that the perpendicular channel is the inlet channel and the lateral channel is the exhaust channel, remains hypothetical. The highly conserved aspartate residues in the perpendicular channel (No. 127 in BLC and No. 181 in HPII) are indicated. The subunit harboring the channels is colored in red and the associated subunit in the dimer is colored green to accentuate its incursion into the perpendicular channel of the red subunit. The two proteins are oriented and scaled in an identical manner for comparison. Figure prepared using SETOR [38].

Acknowledgment

This work was supported by a grant (OGP 9600) from the Natural Sciences and Engineering Research Council (NSERC) of Canada.

References

[1] P. Nicholls, I. Fita, P.C. Loewen, Adv. Inorg. Chem. 51 (2001) 51–106.
[2] M.R.N. Murthy, T.J. Reid III, A. Sicignano, N. Tanaka, M.G. Rossmann, J. Mol. Biol. 152 (1981) 465–499.
[3] I. Fita, A.M. Silva, M.R.N. Murthy, M.G. Rossmann, Acta Crystallogr. B 42 (1986) 497–515.
[4] B.K. Vainshtein, W.R. Melik-Adamyan, V.V. Barynin, A.A. Vagin, A.I. Grebenko, Nature 293 (1981) 411–412.
[5] B.K. Vainshtein, W.R. Melik-Adamyan, V.V. Barynin, A.A. Vagin, A.I. Grebenko, V.V. Borisov, K.S. Bartels, I. Fita, M.G. Rossmann, J. Mol. Biol. 188 (1986) 49–61.
[6] G.N. Murshudov, W.R. Melik-Adamyan, A.I. Grebenko, V.V. Barynin, A.A. Vagin, B.K. Vainshtein, Z. Dauter, K. Wilson, FEBS Lett. 312 (1992) 127–131.
[7] P. Gouet, H.M. Jouve, O. Dideberg, J. Mol. Biol. 249 (1995) 933–954.
[8] J. Bravo, N. Verdaguer, J. Tormo, C. Betzel, J. Switala, P.C. Loewen, I. Fita, Structure 3 (1995) 491–502.
[9] J. Bravo, M.J. Maté, T. Schneider, J. Switala, K. Wilson, P.C. Loewen, I. Fita, Proteins 34 (1999) 155–166.
[10] S. Berthet, L. Nykyri, J. Bravo, M.J. Maté, C. Berthet-Colominas, P.M. Alzari, F. Koller, I. Fita, Protein Sci. 6 (1997) 481–483.
[11] M.J. Maté, M. Zamocky, L.M. Nykyri, C. Herzog, P. Alzari, Betzel, F. Koller, I. Fita, J. Mol. Biol. 286 (1999) 135–139.
[12] T.-P. Ko, M.K. Safo, F.N. Musayev, M.L. Di Salvo, C. Wang, S.-H. Wu, D.J. Abraham, Acta Crystallogr. D 56 (1999) 241–245.
[13] C.D. Putnam, A.S. Arvai, Y. Bourne, J.A. Tainer, J. Mol. Biol. 296 (1999) 295–309.
[14] X. Carpena, R. Perez, W.F. Ochoa, N. Verdaguer, M. Klotz, J. Switala, W. Melik-Adamyan, I. Fita, P.C. Loewen, Acta Crystallogr. D 57 (2001) 1184–1186.
[15] M. Rørth, P.K. Jensen, Biochim. Biophys. Acta 139 (1967) 171–173.

[16] Y. Ogura, Arch. Biochem. Biophys. 57 (1955) 288–300.
[17] E. Layne, Methods Enzymol. 3 (1957) 447–454.
[18] U.K. Laemmli, Nature 227 (1970) 680–685.
[19] K. Weber, J.R. Pringle, M. Osborn, Methods Enzymol. 26 (1972) 3–27.
[20] P.C. Loewen, J. Switala, Biochem. Cell Biol. 64 (1986) 638–646.
[21] J. Switala, O.J. O'Neil, P.C. Loewen, Biochemistry 38 (1999) 3895–3901.
[22] M.G. Klotz, G.R. Klassen, P.C. Loewen, Mol. Biol. Evol. 14 (1997) 951–958.
[23] M. Zamocky, C. Herzog, L.M. Nykyri, F. Koller, FEBS Lett. 367 (1995) 241–245.
[24] S.G. Kalko, J.L. Gelpi, I. Fita, M. Orozco, J. Am. Chem. Soc. 123 (2001) 9665–9672.
[25] P. Amara, P. Andreoletti, H.M. Jouve, M.J. Field, Protein Sci. 10 (2001) 1927–1935.
[26] M.S. Sevinc, M.J. Mate, J. Switala, I. Fita, P.C. Loewen, Protein Sci. 8 (1999) 490–498.
[27] M.R. Mulvey, P.A. Sorby, B.L. Triggs-Raine, P.C. Loewen, Gene 73 (1988) 337–345.
[28] M. Fuangthong, S. Mongkolsuk, FEMS Microbiol. Lett. 152 (1997) 189–194.
[29] E.R. Rocha, C.J. Smith, J. Bacteriol. 177 (1995) 3111–3119.
[30] D. DeShazer, G.E. Wood, R.L. Friedman, Mol. Microbiol. 14 (1994) 123–130.
[31] Z. Sha, T.J. Stabel, J.E. Mayfield, J. Bacteriol. 176 (1994) 7375–7377.
[32] I. Von Ossowski, M.R. Mulvey, P.A. Leco, A. Borys, P.C. Loewen, J. Bacteriol. 173 (1991) 514–520.
[33] S. Odenbreit, B. Wieland, R. Haas, J. Bacteriol. 178 (1996) 6960–6967.
[34] A. Haas, K. Brehm, J. Kreft, W. Goebel, J. Bacteriol. 173 (1991) 5159–5167.
[35] S.M. Brown, M.L. Howell, L. Wasil, A.J. Anderson, D.J. Hassett, J. Bacteriol. 177 (1995) 6536–6544.
[36] M.G. Klotz, Y.C. Kim, J. Katsuwon, A.J. Anderson, Appl. Microbiol. Biotechnol. 43 (1995) 656–666.
[37] G.J. Kleywegt, T.A. Jones, Acta Crystallogr. D 50 (1994) 178–185.
[38] S. Evans, J. Mol. Graphics 11 (1993) 134–138.